OXFORD
SOT | Society of Toxicology
academic.oup.com/toxsci
Tox Spotlight article

TOXICOLOGICAL SCIENCES, 176(1), 2020, 147–161

doi: 10.1093/toxsci/kfaa056
Advance Access Publication Date: April 25, 2020
Research article

Topical Application of the Antimicrobial Agent Triclosan Induces NLRP3 Inflammasome Activation and Mitochondrial Dysfunction

Lisa M. Weatherly,*,[1] Hillary L. Shane,* Sherri A. Friend,† Ewa Lukomska,* Rachel Baur,* and Stacey E. Anderson*

*Allergy and Clinical Immunology Branch and †Pathology and Physiology Research Branch, Health Effects Laboratory Division, National Institute for Occupational Safety and Health, Morgantown, West Virginia 26505

[1]To whom correspondence should be addressed at Allergy and Clinical Immunology Branch, Health Effects Laboratory Division, National Institute for Occupational Safety and Health (NIOSH), 1095 Willowdale Drive, Morgantown, WV 26505. Fax: (304) 285-6126. E-mail: nux6@cdc.gov. **Disclaimer:** The authors alone are responsible for the content of this manuscript. The findings and conclusions in this report are those of the authors and do not necessarily represent the views of the National Institute for Occupational Safety and Health, Centers for Disease Control and Prevention.

ABSTRACT

5-Chloro-2-(2,4-dichlorophenoxy)phenol (triclosan) is an antimicrobial chemical widely used in consumer household and clinical healthcare products. Human and animal studies have associated triclosan exposure with allergic disease. Mechanistic studies have identified triclosan as a mitochondrial uncoupler; recent studies suggest that mitochondria play an important role in immune cell function and are involved in activation of the NLRP3 inflammasome. In this study, early immunological effects were evaluated via NLRP3 activation following dermal triclosan application in a BALB/c murine model. These investigations revealed rapid caspase-1 activation and mature IL-1β secretion in the skin and draining lymph nodes (dLNs) after 1.5% and 3% triclosan exposure. Correspondingly, *pro-Il-1b* and *S100a8* gene expression increased along with extracellular ATP in the skin. Peak gene expression of chemokines associated with caspase-1 activation occurred after 2 days of exposure in both skin tissue and dLNs. Phenotypic analysis showed an increase in neutrophils and macrophages in the dLN and myeloid and inflammatory monocytes in the skin tissue. Triclosan also caused mitochondrial dysfunction shown through effects on mitochondrial reactive oxygen species**, mass, mitochondrial membrane potential, and mitochondrial morphology. These results indicate that following triclosan exposure, activation of the NLRP3 inflammasome occurs in both the skin tissue and dLNs, providing a possible mechanism for triclosan's effects on allergic disease and further support a connection between mitochondrial involvements in immunological responses.**

Key words: triclosan; NLRP3 inflammasome; caspase-1; mitochondria; **allergy**.

Triclosan is a synthetic, broad-spectrum antimicrobial compound used for over 40 years in a wide range of products such as toothpaste, soap, deodorants, body wash, and hand sanitizers (Crinnion, 2010; Dhillon *et al.*, 2015; Fang *et al.*, 2010). Recently, a Food and Drug Administration ruling has led to triclosan being phased out of some products (FDA, 2016). However, triclosan continues to be used in select consumer and clinical healthcare products and formulations (HHS, 2001–2019).

Triclosan has been detected in a variety of human samples including serum, plasma, urine, and breast milk (Allmyr *et al.*, 2006, 2008; Azzouz *et al.*, 2016; Calafat *et al.*, 2008) and in specific tissues including liver, adipose, and brain (Geens *et al.*, 2012; Wang *et al.*, 2015). Multiple epidemiological studies show adverse effects of triclosan on human health (Jackson-Browne *et al.*, 2018; Weatherly and Gosse, 2017; Wei *et al.*, 2017). Exposure has been shown to produce both estrogenic and androgenic outcomes (Ahn *et al.*, 2008; Huang *et al.*, 2014; Stoker *et al.*, 2010), supporting its role as an endocrine-disrupting compound. Epidemiological studies also suggest that triclosan exposure may affect the immune system. A positive association was

demonstrated between triclosan exposure and the diagnosis of hay fever, allergies, and sensitization and exacerbation of food and aeroallergens (Clayton *et al.*, 2011; Savage *et al.*, 2012, 2014; Spanier *et al.*, 2014). Supporting these studies, although not identified as a sensitizing chemical (Anderson *et al.*, 2016), dermal exposure to triclosan augmented the allergic response to ovalbumin (OVA) in a mouse asthma model through a TSLP-mediated pathway (Marshall *et al.*, 2015). Additional research found that this response was initiated through the S100A8/A9-TLR4 pathway (Marshall *et al.*, 2017).

The most common routes of exposure to triclosan are through dermal exposure and ingestion due to its incorporation in skin and oral care products. Triclosan has been demonstrated to be absorbed through the skin in multiple species including human (Moss *et al.*, 2000) and mouse (Kanetoshi *et al.*, 1992). In addition, hospitals using triclosan-containing hand soaps showed an increase in urinary triclosan levels in the healthcare workers (MacIsaac *et al.*, 2014), further supporting the potential for dermal exposure and absorption. Mouse studies have also reported detectable levels of triclosan in numerous tissues following dermal exposure (Fang *et al.*, 2016).

It is known that as the first point of chemical contact, the skin is involved in immune responses and plays a major role in the development of allergic disease. Low molecular weight chemicals can influence allergic disease (Sasseville, 2008) via effects on the skin by inducing danger signals, toll-like receptor (TLR) signaling, and alterations in the skin microbiome (Shane *et al.*, 2019). More recently, a role for the inflammasome has been reported in allergic disease but the specific mechanisms are still being investigated. NLRP3 (NOD-, LRR-, and pyrin domain-containing 3) inflammasome is a cytosolic signaling complex that can respond to multiple stimuli. It is composed of the NLRP3 sensor, the apoptosis-associated speck-like protein containing a CARD (ASC) adaptor molecule, and the procaspase-1 cysteine protease (West *et al.*, 2011). NLRP3 inflammasome activation and elevated IL-1β has recently been linked to the development of allergic disease (Xiao *et al.*, 2018). However, due to the NLRP3 inflammasome's capacity to respond to such a wide array of stimuli, the molecular mechanisms behind the activation are still unknown. Research has demonstrated a role for mitochondria in the activation of the NLRP3 inflammasome (Liu *et al.*, 2018). Investigations into the mechanisms of triclosan toxicity suggest a mitochondrial-based pathway via mitochondrial uncoupling and complex II inhibition (Shim *et al.*, 2016; Teplova *et al.*, 2017; Weatherly *et al.*, 2016, 2018; Zhang *et al.*, 2017). Mitochondria have recently been shown to play important roles in immune cell function through operating as a signaling platform and influencing effects on cell differentiation and activation with subsequent effects on allergic disease (West *et al.*, 2011).

Due to the association of dermal triclosan exposure with allergic disease and mitochondrial function, this study sought to determine whether triclosan could induce NLRP3 inflammasome activation *in vivo* following dermal exposure. The results indicate that dermal exposure of triclosan induces caspase-1 activation and IL-1β secretion in the draining lymph nodes (dLNs) and in the skin. Mitochondrial dysfunction accompanies inflammasome activation in the dLN with morphology changes and decreases in mitochondrial membrane potential (MMP) and organelle mass. These findings demonstrate a connection between mitochondria and immune function following dermal triclosan exposure and support the need for additional research to investigate this association and the immunological impact.

MATERIALS AND METHODS

Animals. Female BALB/cAnNTac (BALB/c) mice were used in these studies. This strain has a T_H2 bias and is commonly used for investigation of allergic disease and has previously been used to investigate the immunological effects of triclosan (Klink and Meade, 2003; Woolhiser *et al.*, 2000). The mice were ordered from Taconic at 6–8 weeks of age and housed 3–5 per cage in ventilated plastic shoebox cages with hardwood ship bedding. Upon arrival, the mice were allowed to acclimate for at least 5 days. Each shipment of animals was randomly assigned to a treatment group. Animals were fed NIH-31 modified 6% irradiated rodent diet with tap water provided from water bottles. A light/dark cycle was maintained on 12-h intervals. Animals were euthanized by CO_2 asphyxiation. All animal experiments were performed in the AAALAC International accredited NIOSH animal facility in accordance with an animal protocol approved by the CDC-Morgantown Institutional Animal Care and Use Committee.

Triclosan exposures. The concentrations of triclosan (Calbiochem; CAS No. 3380-34-5) used in these experiments were determined to be nontoxic and based on findings from previous studies (Marshall *et al.*, 2017). The selected doses also represent translationally-relevant exposure conditions, as triclosan concentrations in products have been reported to range between 0.03% and 1.0% (HHS, 2001–2019).

For all studies, BALB/c mice (5/group) were topically treated with acetone vehicle or increasing concentrations of triclosan (0%–3%) on the dorsal surface of each ear (25 μl/ear) once a day for 1, 2, or 4 consecutive days. Animals were euthanized by CO_2 asphyxiation 24 h after the last exposure. Triclosan has previously been shown to interfere with mitochondrial-specific dyes during direct *in vitro* cell exposure (Weatherly *et al.*, 2018), where the dye is applied to the cells in a buffer that also contains triclosan. In the following *in vivo* studies, triclosan and the mitochondrial dye do not come into direct contact with each other as the animals are exposed to triclosan 24 h before the tissue is processed and then the cells are stained with the dye in triclosan-free buffer.

Tissue collection and processing. Following euthanasia, ears and right and left auricular dLNs were used for subsequent analyses. dLNs were collected in 2-ml sterile phosphate-buffer saline (PBS) (pH 7.4) and single-cell suspensions (2 nodes/animal) were prepared by mechanical disruption of tissues between frosted microscope slides. Ears (2 per mouse; split into ventral and dorsal halves) were collected in RPMI and either used intact or processed into single-cell suspensions prepared by incubating with a 0.25 mg/ml Liberase-TL Research grade (Roche) enzymatic digestion for 90 min at 37°C in RMPI with 100 μg/ml DNase I. Skin tissue was further homogenized using a gentleMACS dissociator (Miltenyi) and passed through a 70-μm cell strainer. Tissue viability and total cellularity was assessed using a Cellometer (Nexcelom) based on acridine orange and propidium iodide incorporation.

Caspase-1 inflammasome activation. Ear and dLN caspase-1 activation was assayed via Promega Caspase-Glo 1 Inflammasome kit according to manufacturer's instructions. Ears (intact; split into dorsal and ventral halves) were incubated for 1.5 h in complete EMEM at 37°C/5% CO_2. Following the 1.5-h incubation supernatants were collected. Following mechanical disruption, the dLN cells were plated at 50 000 cells/well. Caspase-Glo reagent was

prepared according to manufacturer's instructions and added to the plate containing the cells/supernatant. Luminescence was read via plate reader after a 2-h incubation at room temperature. Background luminescence was subtracted and normalized to the corresponding control on each day of the experiment.

Gene expression analysis. Animals were euthanized by CO_2 inhalation 24 h after the final exposure. Left and right ears and left and right auricular dLNs were collected into tubes containing 500 µl RNAlater (Invitrogen) and samples were frozen at −80°C until processed. Tissues were thawed and homogenized with TissueLyser II. Total RNA was isolated from the ear (RNeasy kit) and dLNs (miRNeasy kit) according to the manufacturer's directions (Qiagen). A QIAcube (Qiagen) automated RNA isolation machine was used in conjunction with the specified RNA isolation kit. The concentration and purity of the isolated RNA was determined using a NanoDrop Spectrophotometer (Thermo Scientific). The cDNA synthesis (2000 ng) was performed using Life Technologies high capacity cDNA reverse transcription kit according to manufacturer's recommendations. For analysis of mRNA expression, a reaction of cDNA, TaqMan mouse-specific mRNA primers (Life Technologies), and TaqMan Fast PCR Master Mix (Life Technologies) were added to a MicroAmp Fast Optical 96-well Reaction Plate and analyzed on an Applied Biosystems 7500 Fast Real Time PCR System using default cycling conditions for comparative CT analysis. The mRNA β-actin was used as the endogenous reference. Data were collected and expressed as relative fold change over vehicle control (VC) using the $2^{-\Delta\Delta Ct}$ method.

IL-1β protein assessment. Acetone and triclosan exposed ears and dLNs from BALB/c mice were collected into RPMI and PBS, respectively, following euthanasia. The ears were split into ventral and dorsal halves and incubated intact for 6 h in complete EMEM at 37°C/5% CO_2 to allow time for IL-1β to be secreted. Following the 6-h incubation, supernatants were collected. After mechanical disruption of dLNs, cells were centrifuged, and supernatants were collected. Supernatants from both skin and dLNs were used for IL-1β ELISA according to manufacturer's instructions using Mouse IL-1β Quantikine ELISA Kit (R&D Systems).

Extracellular ATP assay. ATP production was assayed via Promega ToxGlo kit. Acetone and triclosan exposed ears from BALB/c mice were excised and separated into ventral and dorsal halves. Both halves were incubated intact for 1.5 h in complete EMEM at 37°C/5% CO_2 to allow time for ATP to be secreted. After mechanical disruption of dLNs, cells were centrifuged, and supernatants were collected. Supernatants from both skin and dLNs were used to measure extracellular ATP. Luminescence was read via plate reader, background readings were subtracted and normalized to corresponding control on each day of the experiment.

Flow cytometry. For phenotypic analysis, single-cell suspensions of ears and dLNs were resuspended in FACS buffer containing α-mouse CD16/32 antibody (Fc Block) (BD Bioscience) then incubated with a staining cocktail of fluorochrome-conjugated antibodies specific for mouse cell surface epitopes: CD45-BV605 (clone 30-F11), CD11b-PerCP-Cy5.5 (clone M1/70), CD3-PE-CF594 (clone 145-2C11), Ly6G-FITC (clone 1A8) (BD Biosciences); Ly6C-BV421 (HK1.4) (BioLegend); CD169-eF660 (SER-4) (eBiosciences). Cells were then washed, fixed in Cytofix buffer (BD Biosciences) and resuspended in FACS buffer. Events (approximately 1–2 × 10^6/sample) were collected on an LSR II flow cytometer (BD Biosciences) and analyzed using Flowjo software v10.

Mitochondrial mass and mitochondrial reactive oxygen species. For staining of mitochondrial mass (mtMass), single-cell suspensions of dLN were resuspended in 100 µl of 200 nM MitoTracker Green dye in triclosan-free PBS for 20 min at 37°C/5% CO_2. For mitochondrial reactive oxygen species (mtROS), single-cell suspensions of dLN were resuspended in 100 µl of 5 µM MitoSOX Red dye in triclosan-free PBS for 20 min at 37°C/5% CO_2. Cells were washed with PBS, filtered through a 70-µm cell strainer, and resuspended in FACS buffer with 50 µg/ml DNase. Events (approximately 80 000–150 000/sample) were collected on an LSR II flow cytometer (BD Biosciences) and analyzed using Flowjo software v10. All cells were gated on single events followed by lymphocyte gating and lastly gated on either MitoTracker$^+$ or MitoSOX$^+$ cell.

Mitochondrial membrane potential. MMP was measured via MitoProbe JC-1 Assay Kit (ThermoFisher Scientific) according to manufacturer's instructions. Briefly, dLN single-cell suspensions were diluted to 1 × 10^6 cells/ml with a final concentration of 2 µM JC-1 dye in triclosan-free PBS and incubated for 15 min at 37°C/5% CO_2. CCCP was used as a positive control. After 15 min, cells were washed and resuspended in staining buffer. Events (approximately 30 000/sample) were collected on an LSR II flow cytometer using FITC and PE channels of a 488 laser and manually compensated and analyzed using Flowjo software v10. All cells were gated on single events followed by lymphocyte gating. Median fluorescence intensity was measured and normalized to that day's corresponding control.

Transmission electron microscopy. After single-cell preparation, approximately 750 00 dLN cells/sample were fixed with Karnovsky's fixative, postfixed with osmium tetroxide, mordanted in tannic acid, stained with uranyl acetate, alcohol dehydrated, and embedded in Epon. The blocks were sectioned and stained with uranyl acetate and lead citrate. Ultrastructural changes were evaluated using a JEOL JEM-1400Plus transmission electron microscope (JEOL, Tokyo, Japan). Morphometric analyses were performed using NIH Fiji ImageJ with at least 45–60 mitochondria (from at least 10 cells) per concentration. Mitochondria with clearly discernible outlines were manually traced on transmission electron microscopy (TEM) images. Aspect ratio (AR) is defined as [major axis/minor axis]. Circularity [$4\pi \times$ (surface area/perimeter^2)] and roundness [$4 \times$ (surface area)/(π x major axis^2)] are measurement for sphericity where 1 is a perfect sphere. Percent mitochondria that show standard mitochondrial morphology and altered morphology were assessed by defining altered mitochondria as having a fragmented crista, inhomogeneous electron transparent matrix, and/or U-, C-, or ring-shaped morphology.

Whole cell protein lysates. Ears and dLN were collected in 750 µl (ears) and 350 µl (dLN) T-protein extraction reagent (PER) buffer containing protease and phosphatase inhibitor cocktail and EDTA following euthanasia and mechanically disrupted using TissueLyser II in T-PER with protease and phosphatase inhibitor cocktail. The soluble protein fraction was collected and quantified by BCA protein assay (Pierce), according to the manufacturer's instructions.

Capillary western immunoassay. The capillary western immunoassay experiments were performed according to the

Table 1. Primary and Secondary Antibodies Used for ProteinSimple Wes Immunoassay

Antibody	Reference	Sample Concentration	Antibody Dilution	Secondary Antibody
Opa1	Novus Biologicals	0.2 mg/ml (skin)	1:200 (skin)	Anti-rabbit-HRP (Wes detection kit)
	NB-110-55290SS	0.2 mg/ml (dLN)	1:200 (dLN)	
Drp1	Novus Biologicals	0.1 mg/ml (skin)	1:150 (skin)	
	NB110-55288SS	0.1 mg/ml (dLN)	1:150 (dLN)	

ProteinSimple Wes user guide for a 12–230 kDa Separation Module and the Anti-Rabbit detection module. Briefly, prepared skin and dLN lysate samples were diluted to an appropriate concentration in sample buffer then mixed together with fluorescent master mix and incubated at 95°C for 5 min. Appropriate sample concentrations were determined by linear range finding as suggested by the manufacturer, where a range of 0–1 mg/ml of sample was run to determine the lower (limit of detection) and upper (total saturation) detection limits of the assay with a specific antibody. The signal should change in direct proportion to the amount of protein in the sample. Sample concentrations and antibody dilutions are given in Table 1. Experiments were performed in the Wes instrument. Instrument settings used were: stacking and separation at 350 or 375 V for 25–31 min; blocking reagent for 30 min, primary and secondary antibody both for 30 min; luminol/peroxide chemiluminescence detection for approximately 15 min (exposures of 1–2–4–8–16–32–64–128–512 s). The results were inspected to check the automatic peak detection and identification of specific peaks. Criteria used were a peak signal-to-noise ratio above 10 and the peak height/baseline ratio above 3. Area under the curve was determined via Compass Software for Simple Western (ProteinSimple). Total protein was used as a loading control and for normalization.

Statistical analysis. A one-way analysis of variance (ANOVA) was conducted followed by a Dunnett's multiple comparison post-test to compare groups to acetone control. Statistical analyses were performed using Prism GraphPad. Results represent the mean ± SEM of 3–5 mice per group. Results were considered significant at $^{*}p < .05$, $^{**}p < .01$, and $^{***}p < .001$.

RESULTS

Triclosan Activates the NLRP3 Inflammasome In Vivo

Dermal exposure to triclosan has previously been identified to augment the innate immune response (Marshall *et al.*, 2017) and alter mitochondrial function (Shim *et al.*, 2016; Weatherly *et al.* 2016, 2018); therefore, we investigated inflammasome activation. Dermal triclosan exposure induced caspase-1 activation in dLNs after 2 and 4 days (Figure 1A) with significant increases observed at both 1.5% and 3% triclosan exposure. Triclosan also induced caspase-1 activation in the skin after 2 and 4 days of exposure with significant increases observed at both 1.5% (4 days) and 3% (2 and 4 days) (Figure 1B). The increase in luminescence was confirmed to be a result of caspase-1 activation (Supplementary Figure 1). Inflammasome activation usually requires a 2-step process, an initial signal called priming, followed by a second signal called activation. NLRP3 inflammasome activation priming step leads to an increase in *Nlrp3* and *Il-1b* gene expression (He *et al.*, 2016). Therefore, to determine the effect of triclosan exposure on inflammasome priming, *Nlrp3* and *Il-1b* gene expression were investigated. *Nlrp3* mRNA expression increased with triclosan exposure in both the skin and dLN. However, *Nlrp3* expression in the dLN was only significantly upregulated after 2 days of 3% triclosan exposure (Figure 1C). In the skin, *Nlrp3* significantly increased after 2 (approximately 7-fold) and 4 days (approximately 20-fold) of exposure with 3% triclosan (Figure 1D). Interestingly, no increase in *Il-1b* was observed in the dLNs (Figure 2A). However, triclosan induced a drastic increase in *Il-1b* transcript in the skin with a 40-fold increase observed following 2 days of 3% triclosan exposure and over a 100-fold increase (1.5%) and 400-fold increase (3%) compared with acetone control observed by day 4 (Figure 2B). Pro-IL-1β is cleaved by active caspase-1 to produce the mature IL-1β. Mature IL-1β protein secretion was evaluated in the dLNs (Figure 2C) and skin tissue supernatants (Figure 2D). After 1 and 2 days of exposure, a significant increase in IL-1β protein was observed with 3% triclosan in dLNs supernatants and at 2 days with both skin tissue and dLNs supernatants. At 4 days of exposure, IL-1β protein levels were significantly increased following 1.5% and 3% triclosan in dLNs and 3% triclosan in the skin supernatants.

Triclosan Increases Stimuli Associated With NLRP3 Inflammasome Activation

Inflammasome priming and activation can be triggered by danger-associated molecular patterns (DAMPs) (Yang *et al.*, 2019). The small calcium- and zinc-binding protein, S100A8, is considered a DAMP which is released during inflammation (Foell *et al.*, 2007) and has previously been shown to be elevated in response to triclosan exposure (Marshall *et al.*, 2017). Therefore, we investigated whether *S100a8* is increased at an early enough timepoint to contribute to the activation of caspase-1. Gene expression of *S100a8* significantly increased in the dLN following a single exposure with 3% triclosan and continued to increase throughout 4 days of exposure (Figure 3A). In the skin, *S100a8* had an increasing trend in expression at 1 day that reached statistical significance at 2 and 4 days with 3% triclosan. After 4 days of exposure, *S100a8* gene expression was increased over 100-fold with 1.5% triclosan and over 200-fold with 3% (Figure 3B). Previous studies show that S100A8 can act as a priming agent, but alone cannot activate NLRP3, requiring a secondary signal (Goldberg *et al.*, 2017; Simard *et al.*, 2013). ATP can enhance NLRP3 activation and extracellular ATP is also known to provide a secondary activation signal for NLRP3 (Perregaux and Gabel, 1994; Simard *et al.*, 2013). In the skin, extracellular ATP significantly increased after 1 day of exposure and continued to increase throughout 4 days (Figure 3C). At 2 and 4 days of exposure, ATP luminescence values increased to approximately 3 times that of the control. No increase in extracellular ATP was observed in the dLNs (data not shown).

Dermal Triclosan Exposure Leads to Quick Influx of Inflammatory Cells

Triclosan induced a rapid production of chemokine transcripts associated with NLRP3 activation in the dLNs starting as early as 1 (*Ccl19*) and 2 days of exposure (*Cxcl1*, *Cxcl2*, *Ccl2*) (Table 2).

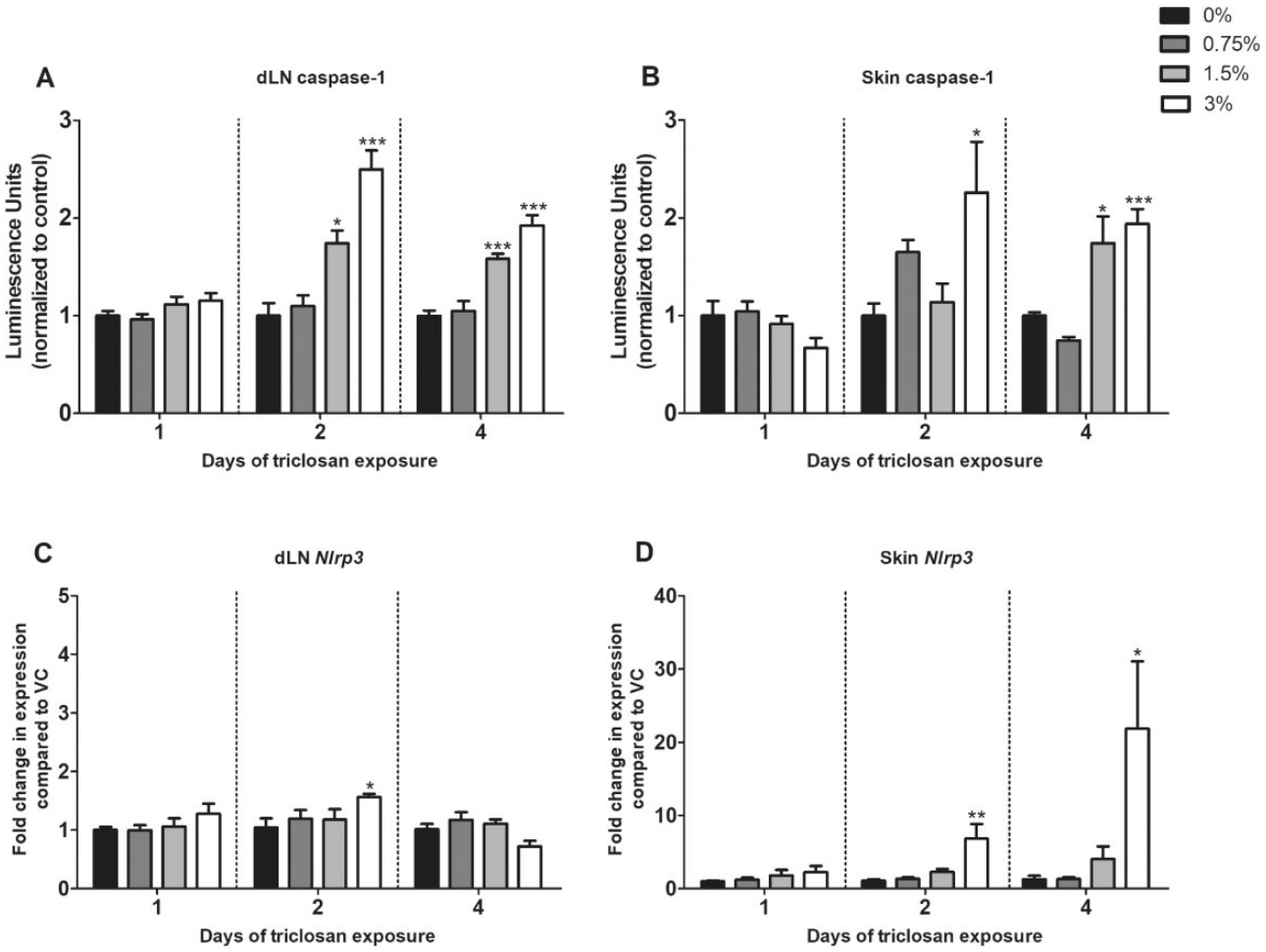

Figure 1. Triclosan activates the NLRP3 inflammasome. Caspase-1 activation was measured in draining lymph nodes (dLNs) (A) and in the skin (B) via luminescence after dermal exposure to 0%, 0.75%, 1.5%, or 3% triclosan for 1, 2, or 4 days. Background luminescence was subtracted followed by normalization to the corresponding days 0% control. Gene expression analysis of *Nlrp3* was performed on dLNs (C) and skin tissue (D) over time following triclosan exposure for up to 4 days. Each point represents the level of *Nlrp3*'s mRNA expression relative to acetone (vehicle control, VC), and normalized to β-actin as an endogenous control. Each concentration represents mean (± SEM) of 5 mice per group. Statistical significance, relative to the corresponding days 0% VC, was determined by one-way ANOVA followed by Dunnett's post-test indicated as $^{*}p < .05$, $^{**}p < .01$, $^{***}p < .001$.

Expression kinetics showed a similar trend for all 4 chemokines, with peak expression at 2 days of exposure. *Cxcl1* and *Ccl19* showed significant increases over time with both 1.5% and 3% triclosan compared with the acetone control. *Cxcl2* (day 2) and *Ccl2* (days 2 and 4) increased with 3% triclosan. Significant increases in $CD45^+$ immune cells were observed after 2 days of triclosan exposure (Table 2). Additional phenotyping identified an increase in the number of $CD11b^+$ myeloid cells after 2 days of triclosan exposure (Table 2). Also, $CD11b^+$ subsets including neutrophils and macrophages increased after 1 day of exposure in the dLNs (Table 2). All these groups continued to increase in cell number after 4 days of exposure with macrophages showing a 6- and 10-fold increase in cell number with 1.5% and 3% triclosan, compared with control.

In the skin, a more dramatic increase in *Cxcl1* and *Cxcl2* expression was observed in the absence of changes in *Ccl2* and *Ccl19* (Table 3). *Cxcl1* expression significantly increased 6-fold following triclosan exposure whereas *Cxcl2* increased over 250-fold compared with control. Both chemokines peaked at 2 days of exposure, however, in the skin a more sustained increase was observed at 4 days with *Cxcl1/2* compared with the dLNs. Phenotypic analysis of the skin identified $CD45^+$ immune cells increased after 4 days of 3% triclosan exposure (Table 3). $CD11b^+$ myeloid cells also increased in the skin after 2 days of exposure (Table 3) along with $CD11b^+Ly6C^+$ inflammatory monocytes (Table 3). These data demonstrate that triclosan is a potent modulator of chemokine release and this chemokine release was associated with rapid innate immune cell infiltration in both the dLNs and the skin, potentially induced by NLRP3 inflammasome activation.

Triclosan Alters Mitochondrial Components in the dLN

In an attempt to examine the mechanisms driving caspase-1 activation, 3 mitochondrial elements (mitochondrial ROS [mtROS], mtMass, and MMP) were investigated in the dLNs. At 2 days, a significant decrease in mtROS was observed with 1.5% and 3% triclosan (Figure 4A). This continued into 4 days where 0.75% triclosan also significantly decreased mtROS. Similar results were observed in dLNs as early as 4 h after exposure (data not shown). An increase in mtROS was detected with *ex vivo* triclosan exposure and T-cell stimulation (data not shown). Next, mtMass was evaluated in the dLNs using MitoTracker. A significant decrease in mtMass occurred after 2 days of exposure with 3% triclosan, continuing into 4 days of exposure (Figure 4B).

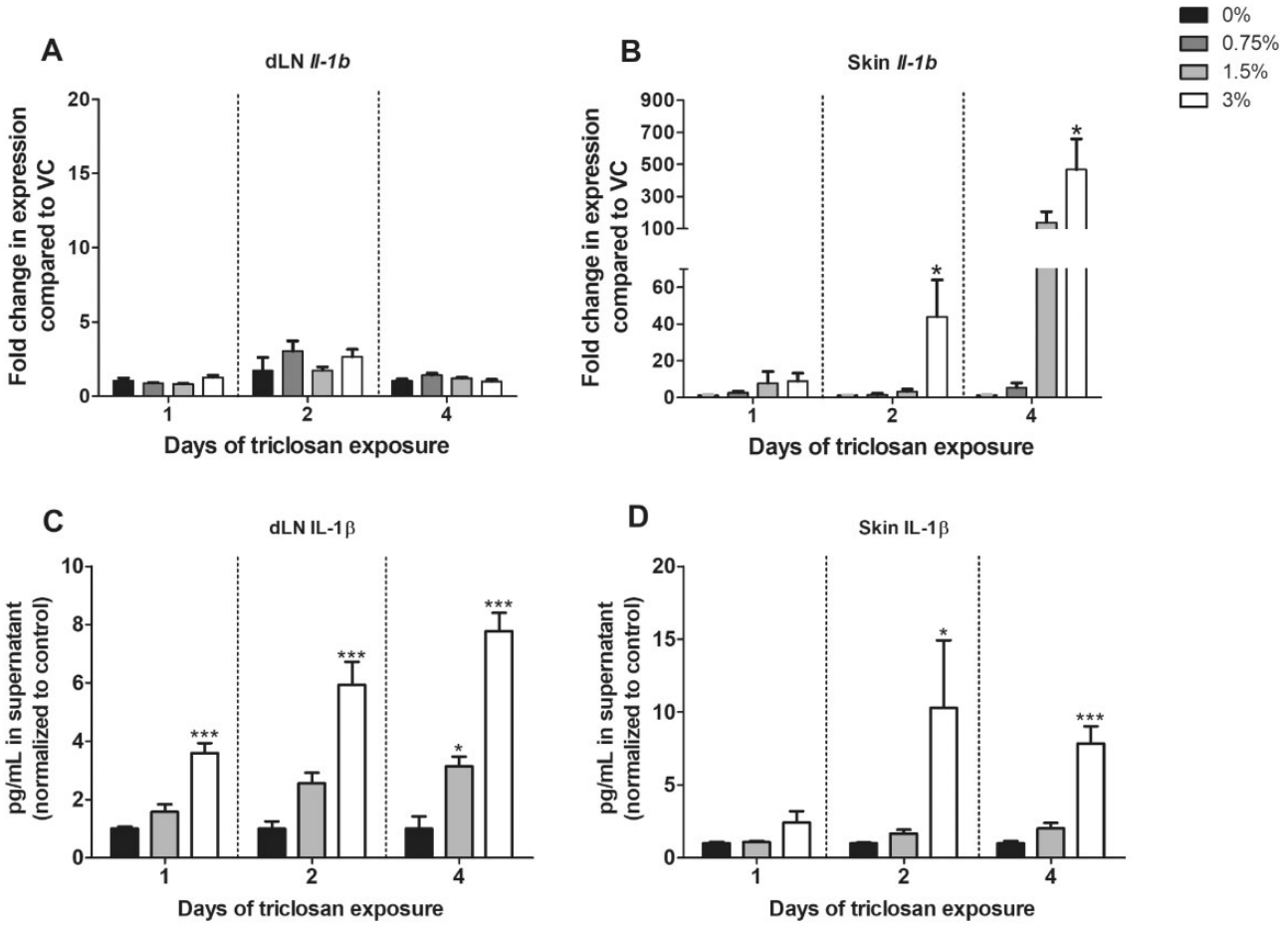

Figure 2. Triclosan increases IL-1β gene and protein expression. IL-1β gene (A, B) and protein expression (C, D) were measured in draining lymph nodes (dLNs) (A, C) and skin tissue (B, D) after dermal exposure to 0%, 0.75%, 1.5%, or 3% triclosan for 1, 2, or 4 days. *Il-1b* mRNA expression is expressed relative to the vehicle control (VC) and normalized to β-actin as an endogenous control. Mature IL-1β protein levels were measured via ELISA from dLNs supernatants (C) and skin tissue supernatants (D) and expressed as pg/ml. Data shown as the mean (± SEM) of 4 and 5 mice per group. Statistical significance, relative to the corresponding days 0% VC, was determined by one-way ANOVA with a Dunnett's post-test where $^{*}p < .05$, $^{***}p < .001$.

MMP was also measured as an indicator of mitochondrial function. Interestingly, the MMP quickly decreased after 1 day of exposure with all triclosan concentrations (Figure 4C). At 2 days of exposure, 1.5% and 3% triclosan still induced a decrease in MMP. By 4 days, MMP had completely recovered with no significant decrease due to triclosan. CCCP was used as a positive control for MMP depolarization with CCCP decreasing MMP to around 20% of the control (data not shown).

Triclosan Induces Mitochondrial Morphology Changes in the dLN

mtMass was most significantly decreased after 4 days of triclosan exposure; therefore, mitochondrial morphology was evaluated after 4 days of triclosan exposure via TEM to investigate if the decrease in mtMass was due to a change in morphology. TEM images of control mitochondria displayed normal morphology with intact membranes and cristae (Figs. 5A–C). Triclosan exposed (4 days) mitochondria appeared swollen and showed disrupted cristae with inhomogeneous electron transparent matrix (Figs. 5D–G). Appearances of mitochondria U-, C-, or ring-shaped morphology were observed in the triclosan-exposed mice (Figs. 5H–K), however, none of these morphologies were seen with control mitochondria. Upon analysis, triclosan exposure also induced an increase in circularity and roundness and a decrease in AR with 0.75%, 1.5%, and 3% exposure (Figs. 5L–N). These findings suggest triclosan is inducing mitochondrial fission in the dLNs. When standard mitochondria and altered mitochondria were analyzed (see Materials and Methods section for parameters), control cells had mitochondria with approximately 90% standard morphology and only 10% with an altered morphology (Figure 5O). The percentage of standard mitochondria decreased with an increase in triclosan concentration, with standard mitochondria decreasing to approximately 50% and increasing altered mitochondria to approximately 50% with 3% triclosan exposure.

To further investigate whether mitochondrial fission occurs with triclosan exposure, mitochondrial fusion and fission proteins were assessed. Dynamin-related protein 1 (Drp1) is required for mitochondrial fission (Fonseca *et al.*, 2019) and an increase in Drp1 can lead to an increase in mitochondrial fission. Optic atrophy 1 (Opa1) mediates fusion of the inner mitochondrial membrane (El-Hattab *et al.*, 2018). A representative virtual blot image with dLN lysates is shown in Figure 5P. A Drp1 band in dLN was observed at 80 kDa and Opa1 band at around 92 kDa (Figure 5P). No additional cleavage in Opa1 was seen after 4 days of triclosan exposure, but bands at 64 and 76 kDa did appear after 7 days of exposure (data not shown).

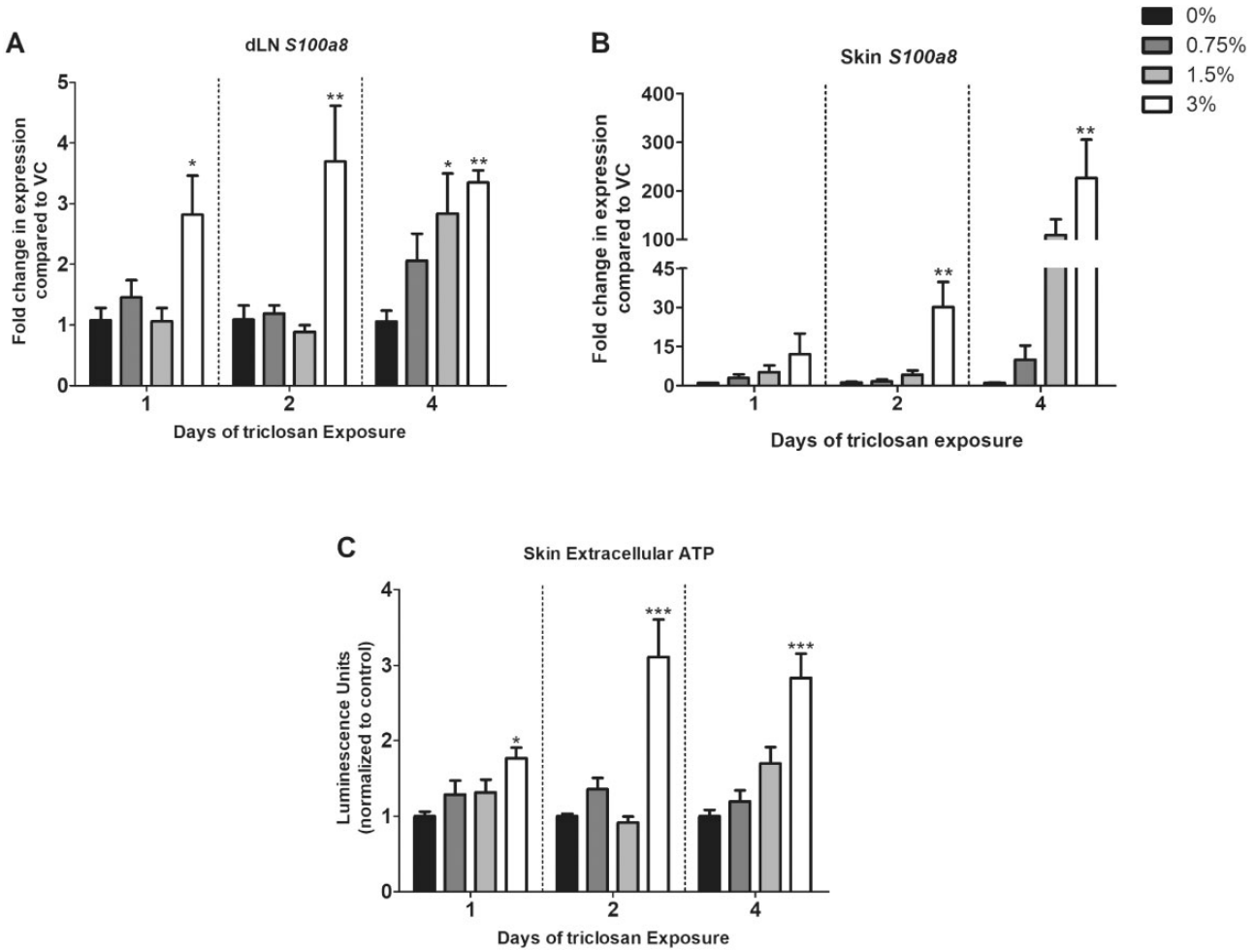

Figure 3. Extracellular ATP and *S100a8* gene expression increase with triclosan exposure. Gene expression in the draining lymph node (dLN) (A) and skin (B) and ATP in the skin (C) were measured after dermal exposure to 0%, 0.75%, 1.5%, or 3% triclosan for 1, 2, or 4 days. *S100A8* mRNA expression is expressed relative to the acetone vehicle control (VC) and normalized to β-actin for normalization as an endogenous control. Extracellular ATP was measured via luminescence from tissue supernatant. Background luminescence was subtracted followed by normalization to the corresponding days 0% control. Data shown as the mean (± SEM) of 4 and 5 mice per group. Statistical significance relative to the corresponding days 0% VC determined by one-way ANOVA followed by Dunnett's post-test indicated as $^{*}p < .05$, $^{**}p < .01$, $^{***}p < .001$.

Upon analysis, Drp1 protein increased in a dose-response manner with a significant increase with 3% triclosan (Figure 5Q). Opa1 protein expression decreased with 1.5% and 3% triclosan exposure compared with control (Figure 5R). Total protein was used for normalization and as a loading control, wherein no change in total protein was seen between concentrations (Supplementary Figure 4). These experiments were repeated in the skin at site of exposure to determine if similar effects were occurring. A representative virtual blot is shown in Figure 5S. In the skin, there was no significant change in Drp1 protein expression (Figure 5T), but there was a decrease in Opa1 with 1.5% and 3% triclosan (Figure 5U), similar to what was observed in the dLNs. These data indicate an imbalance in the mitochondrial fusion and fission machinery with triclosan exposure and support the TEM images, suggesting that triclosan exposure results in mitochondrial fragmentation *in vivo*.

DISCUSSION

The incidence of allergic disease continues to increase worldwide (Ruby Pawankar *et al.*, 2012). Although many chemicals are known to directly influence allergic disease (Folletti *et al.*, 2017; Hong *et al.*, 2014), some including triclosan can induce immunomodulatory effects that can indirectly affect allergic response/hypersensitivity (Anderson *et al.*, 2013, 2016; Marshall *et al.*, 2015). The mechanisms of allergic diseases are continually being investigated and mediators elucidated. Therefore, the studies described in this manuscript were undertaken to better define the immunomodulatory effects of triclosan through investigations of NLRP3 inflammasome activation and mitochondrial dysfunction.

The inflammasome complex is a multiprotein oligomer which contains proteins of the NLR family. By sensing danger and consequently activating caspase-1, certain NLRs facilitate the processing of prointerleukin IL-1β and other proinflammatory cytokines (Evavold and Kagan, 2018). NLRP3 is the most comprehensively studied NLR and evidence suggests that the inflammation resulting from NLRP3 activation is critical for the development of allergic disease (Besnard *et al.*, 2011).

Currently, a 2-step process is widely accepted for NLRP3 activation. TLR activation via PAMPs or DAMPs is considered the first step or priming and leads to an increase in *pro-Il-1b* and *Nlrp3* transcription. Step 2 promotes the association and

Table 2. dLN Chemokine Expression and Cellular Phenotyping Following Dermal Triclosan Exposure

Exposure Duration	1 Day				2 Days				4 Days			
Triclosan (w/v)	0%	0.75%	1.5%	3%	0%	0.75%	1.5%	3%	0%	0.75%	1.5%	3%
Cxcl1 (fold change)	1.01 ± 0.09	0.95 ± 0.06	1.31 ± 0.21	1.53 ± 0.27	1.01 ± 0.06	1.65 ± 0.31	1.68 ± 0.19*	2.32 ± 0.13***	1.02 ± 0.11	1.22 ± 0.20	1.43 ± 0.19	1.27 ± 0.09
Cxcl2 (fold change)	1.02 ± 0.12	1.12 ± 0.08	1.35 ± 0.18	1.67 ± 0.25	1.02 ± 0.11	1.44 ± 0.22	1.67 ± 0.18	2.30 ± 0.34**	1.02 ± 0.09	1.15 ± 0.13	1.54 ± 0.25	1.32 ± 0.11
Ccl2 (fold change)	1.00 ± 0.04	1.08 ± 0.16	1.02 ± 0.11	1.46 ± 0.34	1.11 ± 0.24	1.69 ± 0.28	1.62 ± 0.22	2.07 ± 0.29*	1.00 ± 0.03	1.23 ± 0.16	1.33 ± 0.09	1.62 ± 0.13**
Ccl19 (fold change)	1.00 ± 0.06	0.86 ± 0.09	1.38 ± 0.05	1.46 ± 0.22*	1.03 ± 0.13	1.46 ± 0.14	1.97 ± 0.10*	2.42 ± 0.37***	1.02 ± 0.12	1.33 ± 0.12	1.58 ± 0.16*	1.72 ± 0.11**
$CD45^+$ ($\times 10^6$)	1.62 ± 0.10	1.57 ± 0.17	1.30 ± 0.10	1.96 ± 0.22	1.57 ± 0.38	1.78 ± 0.19	1.63 ± 0.33	3.38 ± 0.54*	1.87 ± 0.09	1.67 ± 0.19	3.22 ± 0.27**	4.76 ± 0.28***
$CD11b^+$ ($\times 10^4$)	5.49 ± 0.38	4.89 ± 0.35	5.12 ± 0.41	6.86 ± 0.70	4.23 ± 0.86	4.72 ± 0.54	4.10 ± 0.97	10.30 ± 1.29**	7.62 ± 0.57	5.83 ± 0.46	11.20 ± 0.96*	15.70 ± 0.88***
Macrophages ($\times 10^4$)	0.34 ± 0.03	0.35 ± 0.47	0.45 ± 0.53	1.10 ± 0.19***	0.23 ± 0.05	0.38 ± 0.05	0.49 ± 0.13	2.10 ± 0.33***	0.39 ± 0.03	0.44 ± 0.04	2.40 ± 0.21***	4.17 ± 0.20***
Neutrophils ($\times 10^3$)	0.79 ± 0.01	1.23 ± 0.09	0.98 ± 0.07	2.71 ± 0.63**	0.63 ± 0.25	1.29 ± 0.40	0.78 ± 0.06	3.20 ± 0.66**	1.28 ± 0.26	0.87 ± 0.08	2.13 ± 0.16	3.02 ± 0.33***

Data shown as the mean (± SEM) of 5 mice per group. Statistical significance relative to the corresponding days 0% VC determined by one-way ANOVA followed by Dunnett's post-test indicated as $^*p < .05$, $^{**}p < .01$, $^{***}p < .001$. Representative flow plots showing the identification of $CD11b^+$ subgroups are shown in Supplementary Figure 2.

Table 3. Skin Chemokine Expression and Cellular Phenotyping Following Dermal Triclosan Exposure

Exposure Duration	1 Day				2 Days				4 Days			
Triclosan (w/v)	0%	0.75%	1.5%	3%	0%	0.75%	1.5%	3%	0%	0.75%	1.5%	3%
Cxcl1 (fold change)	1.03 ± 0.12	2.19 ± 0.31	2.09 ± 0.23	3.41 ± 1.18	1.13 ± 0.30	1.23 ± 0.33	1.76 ± 0.45	6.05 ± 1.45**	1.14 ± 0.30	0.99 ± 0.10	2.12 ± 0.35	5.19 ± 1.93*
Cxcl2 (fold change)	1.03 ± 0.68	7.61 ± 5.67	25.68 ± 20.57	26.54 ± 14.35	1.40 ± 0.54	11.64 ± 9.65	17.66 ± 7.40	265.64 ± 107.09**	1.79 ± 0.90	1.84 ± 0.73	13.28 ± 3.45	222.43 ± 105.17*
Ccl2 (fold change)	1.06 ± 0.18	0.58 ± 0.06	0.82 ± 0.08	1.28 ± 0.26	1.01 ± 0.09	1.17 ± 0.16	1.49 ± 0.17	2.12 ± 0.67	1.38 ± 0.64	0.61 ± 0.05	0.83 ± 0.09	1.01 ± 0.39
Ccl19 (fold change)	1.05 ± 0.20	0.94 ± 0.13	1.21 ± 0.17	1.27 ± 0.21	1.01 ± 0.90	1.21 ± 0.22	1.49 ± 0.14	1.76 ± 0.27	1.18 ± 0.40	0.78 ± 0.07	0.88 ± 0.10	0.59 ± 0.07
$CD45^+$ ($\times 10^5$)	2.57 ± 0.30	2.46 ± 0.42	2.65 ± 0.18	2.68 ± 0.33	2.51 ± 0.18	2.33 ± 0.22	2.74 ± 0.21	3.22 ± 0.38	2.40 ± 0.09	2.54 ± 0.20	3.13 ± 0.18	4.94 ± 1.00**
$CD11b^+$ ($\times 10^5$)	1.27 ± 0.17	1.22 ± 0.32	1.35 ± 0.98	1.37 ± 0.17	1.38 ± 0.07	1.34 ± 0.14	1.51 ± 0.15	2.24 ± 0.35*	1.20 ± 0.05	1.32 ± 0.10	1.69 ± 0.10*	2.16 ± 0.22***
$CD11b^+Ly6C^+$ ($\times 10^4$)	1.07 ± 0.34	1.03 ± 0.09	1.22 ± 0.10	1.71 ± 0.24	0.94 ± 0.09	1.92 ± 0.65	2.17 ± 0.48	9.43 ± 0.30**	1.02 ± 0.06	1.27 ± 0.10	3.58 ± 0.56	9.07 ± 2.39***

Data shown as the mean (± SEM) of 5 mice per group. Statistical significance relative to the corresponding days 0% VC determined by one-way ANOVA followed by Dunnett's post-test indicated as $^*p < .05$, $^{**}p < .01$, $^{***}p < .001$. Representative flow plots showing the identification of $CD11b^+$ and $CD11b^+Ly6C^+$ inflammatory monocytes are shown in Supplementary Figure 3.

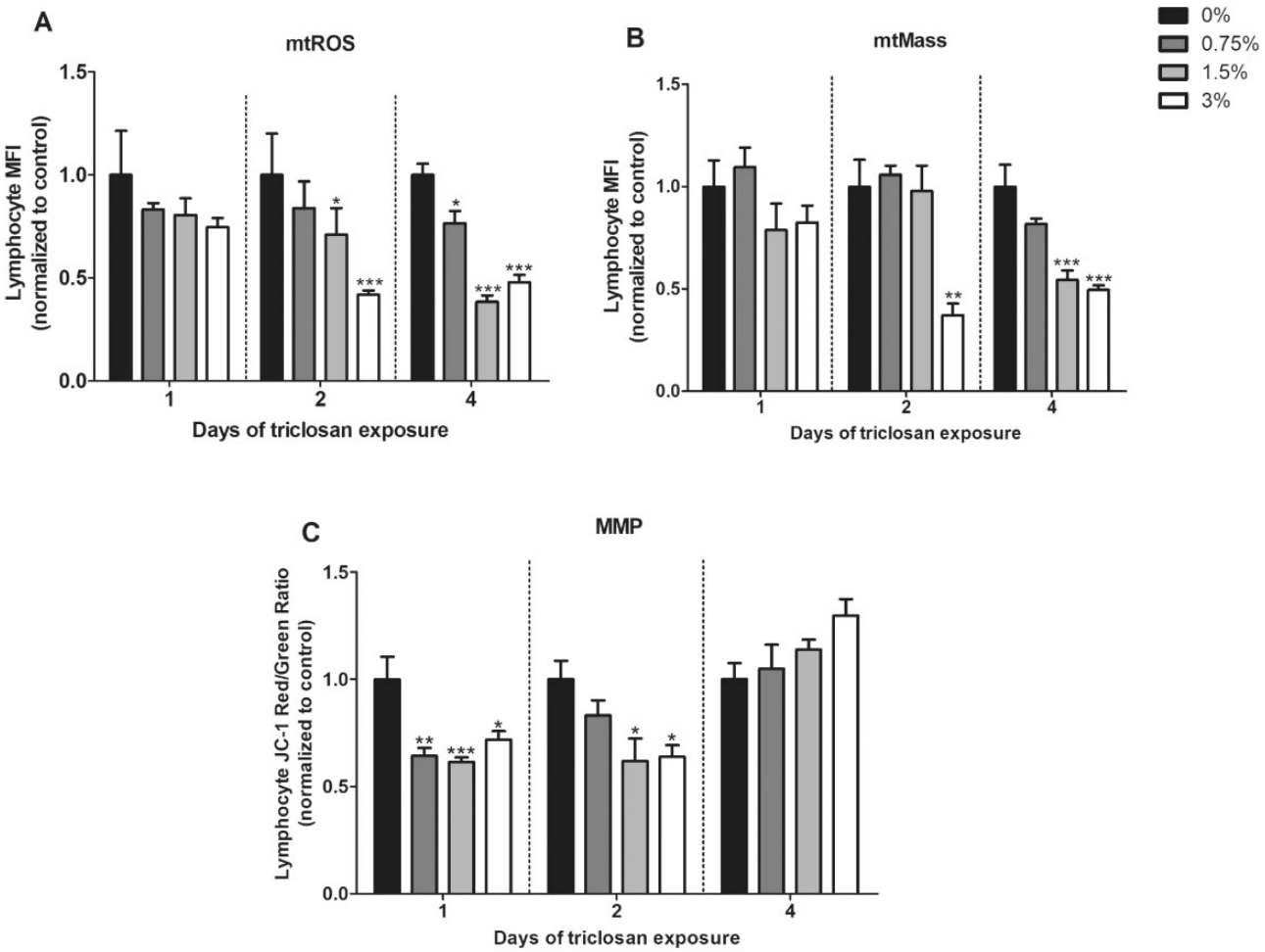

Figure 4. Triclosan alters mitochondrial components in skin draining lymph nodes (dLNs). Mitochondrial ROS (mtROS) (A), mitochondrial mass (mtMass) (B), and mitochondrial membrane potential (MMP) (C) were measured in lymphocytes from dLNs after dermal exposure to triclosan via 5 μM MitoSOX Red, 200 nM MitoTracker Green FM, and 2 μM JC-1, respectively. Using flow cytometry, median fluorescence intensity (MFI) was measured and normalized to the days corresponding 0% vehicle control (VC) (A, B). JC-1 dye undergoes a spectral shift upon depolarization and was analyzed via a red/green fluorescence intensity ratio (C). Data shown as the mean (± SEM) of 5 mice per group. Statistical significance relative to the days corresponding 0% VC determined by one-way ANOVA followed by Dunnett's post-test indicated as $^{*}p < .05$, $^{**}p < .01$, $^{***}p < .001$.

initiation of the NLRP3 inflammasome assembly and is caused by multiple stimulators (Yu and Lee, 2016). Complex assembly results in activation of caspase-1 (Thornberry *et al.*, 1992). Activated caspase-1 can then cleave pro-IL-1β and pro-IL-18 to their mature active forms (Gu *et al.*, 1997; Thornberry *et al.*, 1992). Here, we show that dermal application of triclosan can induce NLRP3 inflammasome activation in mice (Figs. 1A and 1B). An increase in *Nlrp3* (Figs. 1C and 1D) and *Il-1b* mRNA (Figs. 2A and 2B) was only observed in the skin after triclosan exposure, however, secreted mature IL-1β protein increased in both the skin and dLN (Figs. 2C and 2D). Although an increase in caspase-1 activation is expected because it acts upstream of IL-1β, in the dLN, an increase in mature IL-1β was observed at day 1 without a significant increase in caspase-1 activation. One possible explanation for this finding is assay sensitivity. Caspase-1 was evaluated via luminescence-based plate reader assay (versus the ELISA IL-1β assay) which may not be sensitive enough to detect small increases in activation. However, there was as increasing trend (Linear Trend Test $p = .0525$) in caspase-1 activity at day 1 postexposure in the dLN.

Some research has suggested that inflammasome activation does not occur in mouse keratinocytes (Sand *et al.*, 2018) and that infiltrating myeloid cells are responsible for secreting IL-1β in the skin (Drexler *et al.*, 2012). In this study, an increase in $CD11b^{+}$ myeloid cells occurred in the skin along with an increase in inflammatory monocytes (Table 3); these cell populations could be responsible for the caspase-1 activation. Even though there is caspase-1 activation in the dLN without increases in *Il-1b* and *Nlrp3* mRNA, suggesting a lack of priming, phenotypic analysis of the dLN show $CD11b^{+}$ myeloid cells increased along with macrophages and neutrophils after triclosan exposure (Table 2). It is plausible that the cells in the dLN could begin to be "primed" at the site of exposure in the skin then migrate into the dLN as the timing of caspase-1 activation in the dLN coincides with migration of macrophages from the skin seen previously (Toichi *et al.*, 2008). In addition, IL-1β protein was increased in the dLN.

Although many different stimuli including Ca^{2+} signaling, ROS production, mitochondrial DNA release, and extracellular ATP, have been shown to activate NLRP3, a direct ligand for this inflammasome has yet to be identified (Groslambert and Py, 2018; Pedra *et al.*, 2009). In this study, triclosan induced both a priming and activation signal in the skin, as evidenced by a

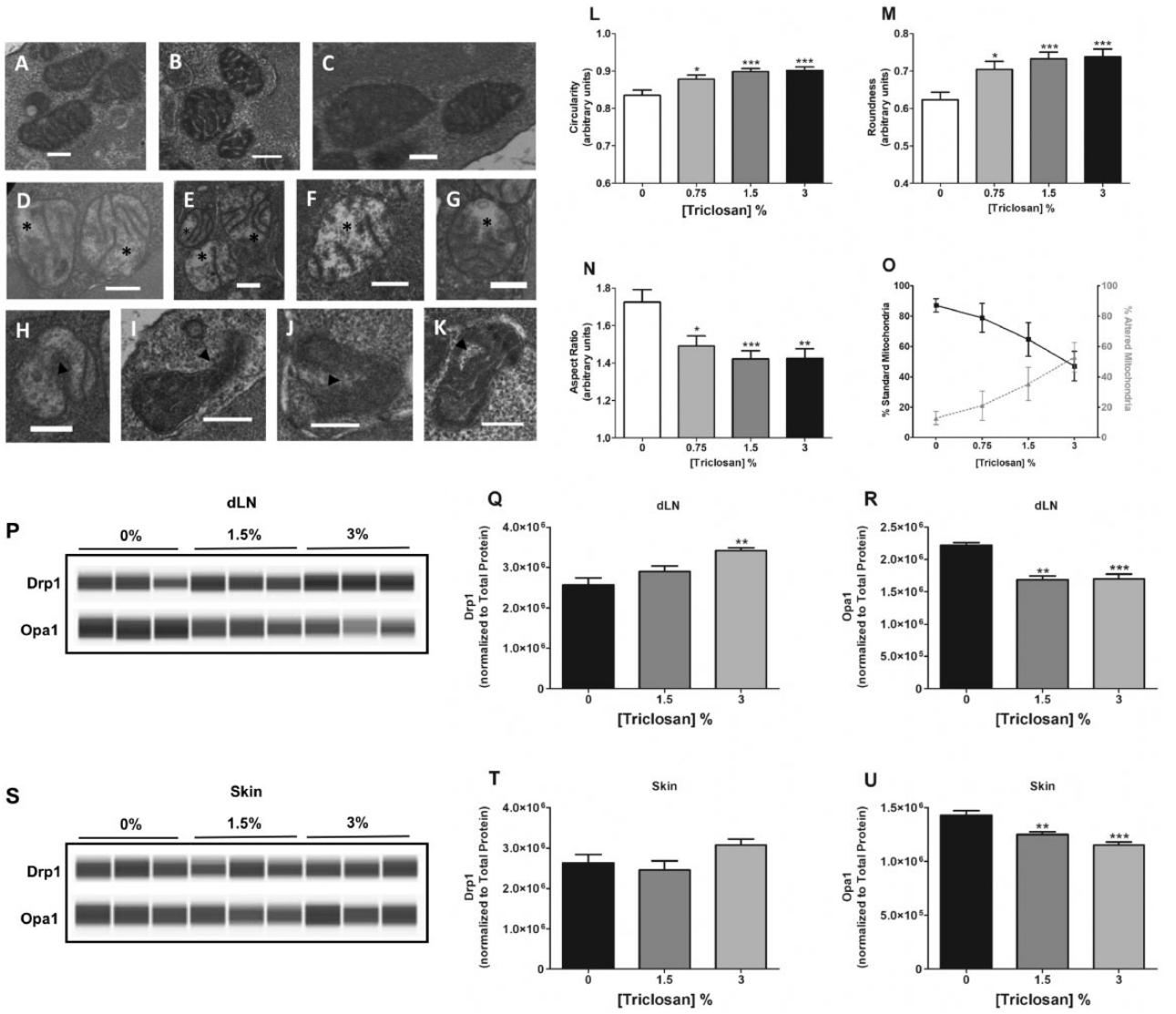

Figure 5. A–O, Triclosan induces mitochondrial morphology changes in draining lymph node (dLN) cells. Mitochondrial morphology in dLN cells was examined by transmission electron microscopy after dermal exposure to 0% (A–C), 0.75% (D, H), 1.5% (E, I), or 3% (F, G, J, K) triclosan for 4 days. Representative images of triclosan-exposed mitochondria show signs of damage (D–G) as indicated by fragmented mitochondria and inhomogeneous electron transparent matrix (asterisk). Triclosan also induced a change in morphology with U-, C-, or ring-shaped mitochondria (H–K) (arrow head). Scale bars = 250 nm. Morphometric analyses (n = at least 45 mitochondria) were done via Fiji ImageJ measuring mitochondrial circularity (L), roundness (M), and aspect ratio (N). Percent mitochondria that show standard mitochondrial morphology and altered morphology was assessed by defining altered mitochondria as having a fragmented crista, inhomogeneous electron transparent matrix, and/or U-, C-, or ring-shaped morphology (O). P–U, Triclosan alters fusion and fission protein levels. Dynamin-related protein 1 (Drp1) and optic atrophy 1 (Opa1) protein levels were analyzed via ProteinSimple Wes Immunoassay system. Virtual blot view of Wes results showing the Drp1 and Opa1 levels obtained in dLN lysates after 4 days of triclosan exposure (P). Area under the curve (AUC) analysis of Drp1 (Q) and Opa1 (R) with normalization to total protein. Virtual blot view of Wes results showing the Drp1 and Opa1 levels obtained in skin tissue lysates after 4 days of triclosan exposure (S). AUC analysis of Drp1 (T) and Opa1 (U) with normalization to total protein. Data shown as the mean (± SEM) of 3–5 mice per group. Statistical significance relative to 0% vehicle control determined by one-way ANOVA followed by Dunnett's post-test indicated as $^{**}p < .01$, $^{***}p < .001$.

drastic increase in *S100a8* gene expression accompanied by an increase in extracellular ATP (Figs. 3B and 3C). However, in the dLN, there was an increase in *S100a8* mRNA (Figure 3A) but no effects on extracellular ATP (data not shown). Contrary to what has been demonstrated *in vitro*, *in vivo* experiments show intraperitoneal LPS alone (without a secondary ATP signal) can lead to NLRP3 inflammasome activation (He *et al.*, 2013; Mariathasan *et al.*, 2006). It is unclear whether ATP is required for LPS-induced IL-1β production or if other cell types provide the ATP required for *in vivo* activation. Both S100A8 and extracellular ATP could be providing the necessary signals for NLRP3 activation, both of which were induced following dermal triclosan exposure.

Inflammasome activation is critical for recruitment of immune cells and mediators (Boro and Balaji, 2017; Sharma and Kanneganti, 2016). In these studies, triclosan increased expression of the chemokines *Cxcl1/2*, *Ccl2*, and *Ccl19* in the dLN (Table 2) and *Cxcl1/2* in the skin (Table 3). An increase in *Cxcl2*, *Ccl2*, and *Ccl19* in the lymph node has previously been shown to be due to the presence of caspase-1, where caspase-1 deficient mice showed a reduction in expression compared with wild type after viral infection (Sagoo *et al.*, 2016). Another study

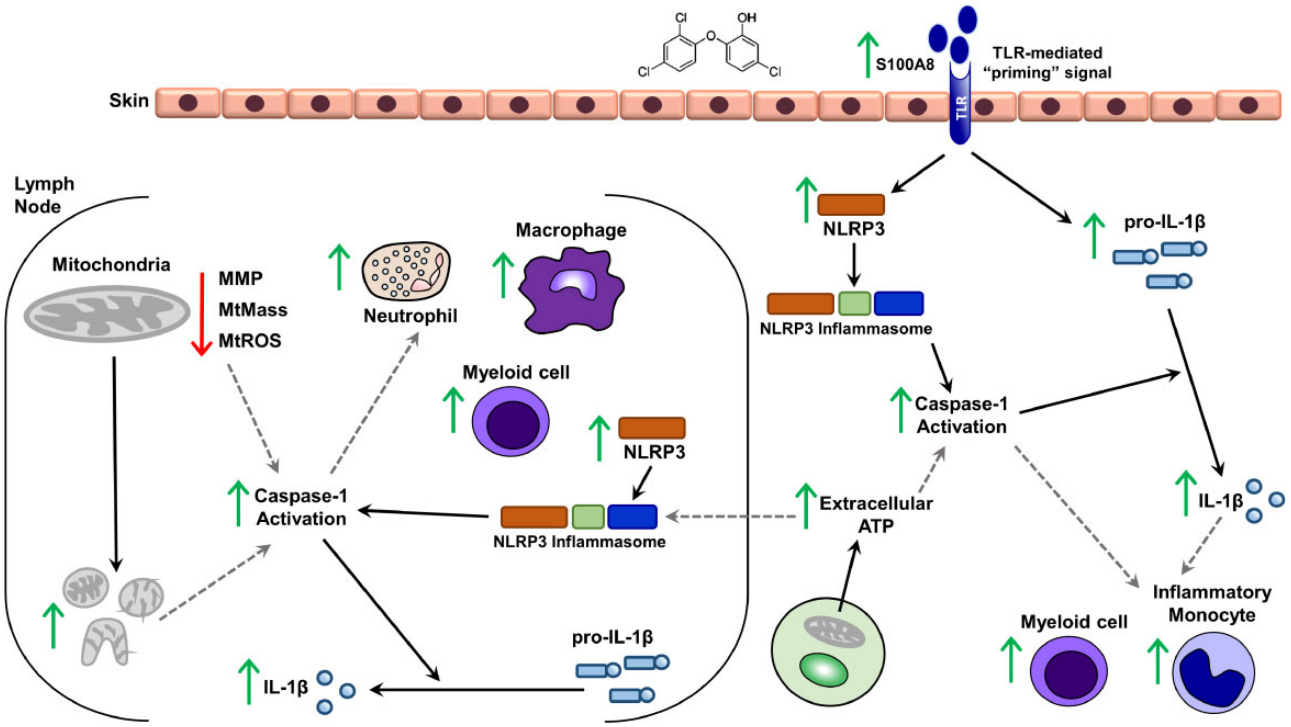

Figure 6. Schematic of the effects of dermal triclosan exposure on the skin and draining lymph node (dLN) in a BALB/c mouse model. Dermal triclosan exposure increases *S100a8* gene expression in the skin causing toll-like receptor signaling activation leading to an increase in *Nlrp3* and *pro-Il-1b* gene expression (priming signal). An increase in extracellular ATP occurs in the skin upon triclosan exposure, possibly acting as a secondary signal leading to caspase-1 activation. Active caspase-1 then cleaves pro-IL-1β leading to an increase in its active form. The activation of caspase-1 and subsequent cleavage of IL-1β could be responsible for the increase in myeloid and inflammatory monocyte cells migrating into the skin. Caspase-1 activation also occurs in the dLN with an increase in mature IL-1β secretion. Myeloid cells, neutrophils, and macrophages increase in number in the dLN, possibly migrating due to the caspase-1 activation. Triclosan also caused a decrease in mitochondrial mass, mitochondrial ROS, and mitochondrial membrane potential in the dLN with an increase in altered mitochondria. Upward facing arrows indicate an increase found in this study and the downward facing arrows indicate a decrease. Dotted arrows/lines are effects suggested in the literature. Abbreviations: Drp1, dynamin-related protein 1; Opa1, optic atrophy 1.

showed blockage of *Cxcl1/2* can reduce IL-1β production and *Cxcl1* can strengthen NLRP3 activation (Boro and Balaji, 2017). The increase in these chemokines further supports NLRP3 inflammasome activation.

Triclosan has previously been demonstrated to be a mitochondrial uncoupler (Shim *et al.*, 2016; Weatherly *et al.*, 2016) which supports the potential for immunological effects regulated via ATP. Although no decrease in intracellular ATP was observed in this study in dLNs (data not shown), intracellular ATP could not be measured in skin tissue due to the intense processing requirements. However, certain studies have shown intracellular ATP production to be independent of NLRP3 activation (Heid *et al.*, 2013). Triclosan alters oxidative phosphorylation and diverse cell types within a single tissue rely on different forms of energy production (Pearce *et al.*, 2013); therefore, certain cell types could be more susceptible to the metabolic effects of triclosan, but unfortunately, individual cell populations were not evaluated in this study.

Mitochondrial dysfunction is also hypothesized to be a trigger for NLRP3 activation. Our studies demonstrated a very drastic decrease in mtROS production, when examined at both 4 h postexposure (data not shown) and 24 h postexposure (Figure 4A). Although an increase in mtROS is thought to be required for caspase-1 activation (Abais *et al.*, 2015; Martinon, 2010), a cardiolipin dependent pathway has also been shown to lead to caspase-1 activation and IL-1β release, independent of mtROS production (Iyer *et al.*, 2013). Studies have also shown that mtROS production is transient (Benani *et al.*, 2007; Fedoseeva *et al.*, 2017; Zorov *et al.*, 2006); therefore, the decrease seen in this study could be due to the timing between exposure and mtROS measurement. In previous studies, triclosan exposure induced pro-oxidative stress (Szychowski *et al.*, 2016; Tamura *et al.*, 2012; Yueh *et al.*, 2014; Zhang *et al.*, 2018) with increases *in vitro* in intracellular ROS (Weatherly *et al.*, 2018) and mtROS (Zhang *et al.*, 2017) occurring very quickly (less than 1 h) upon exposure. In addition, due to the previously described processing requirements, mtROS could not be examined in the skin in this study; it is possible that transient increases in mtROS occur at early timepoints in the skin. It is also possible that the decrease in mtROS is due to lymphocyte activation as T cells are known to switch from oxidative phosphorylation to glycolysis upon activation (van der Windt and Pearce, 2012). However, triclosan has only been shown to activate cells with an additional antigen being present (Marshall *et al.*, 2015; Palmer *et al.*, 2012). After only a single dose, triclosan also induced depolarization of the inner mitochondrial membrane (MMP) in the dLN; the MMP recovered to baseline levels after 4 days of triclosan exposure (Figure 4C). Recent studies suggest that mitochondrial depolarization occurs independently of NLRP3 inflammasome activation (Munoz-Planillo *et al.*, 2013; Won *et al.*, 2015); however, mitochondrial damage has been shown to cause a positive feedback loop with inflammasome activation (Liao *et al.*, 2019). Thus, effects on MMP are still important in the understanding of the inflammasome pathway.

Further investigation into triclosan effects *in vivo* showed disrupted mitochondrial morphology in the dLN (Figure 5)

which has been associated with exposure to other mitochondrial uncouplers (Ding *et al.*, 2012; Giedt *et al.*, 2012) and observed *in vitro* with triclosan exposure (Weatherly *et al.*, 2018), but have never before been demonstrated *in vivo* with triclosan exposure. The result also suggests disruption of the mitochondrial fusion/fission balance (Figure 5). Opa1 is involved in the control of cristae morphology (Del Dotto *et al.*, 2018; Merkwirth and Langer, 2009), and therefore, the decrease in Opa1 protein levels occurring following triclosan exposure could be contributing to both the increase in fragmented mitochondria and the disruption of the mitochondrial cristae. Mitochondrial dynamics (fusion and fission) control mtMass (Chao *et al.*, 2017), which decreased following exposure (Figure 4B). Both cell swelling (Compan *et al.*, 2012), Opa1-mediated fusion and Drp1-mediated fission (Li *et al.*, 2016; Liu *et al.*, 2015) have been suggested to help promote NLRP3 activation; supporting another connection between triclosan's mitochondrial toxicity and inflammasome activation. However, others have found that increased fusion-activated NLRP3 inflammasome (Park *et al.*, 2015). *In vitro*, different methods of activation show disparities in activation of NLRP3 (Won *et al.*, 2015; Zhou *et al.*, 2011) even with the same chemical (Park *et al.*, 2015; Wang *et al.*, 2014; Zhou *et al.*, 2011). In general, the ability of chemicals to activate NLRP3 seems to rely on their capacity to alter more than one cellular process.

In summary, this study suggests that NLRP3 inflammasome activation occurred in the skin and dLN leading to IL-1β release as well as inducing mitochondrial dysfunction in triclosan-exposed mice (Figure 6). These findings provide additional insight into the mechanisms of action following dermal triclosan exposure, demonstrate a connection between mitochondria and immune function, and support the need for additional research to investigate this association and the immunological impact. Evaluation of mechanisms involving novel mediators, such as the ones described in this manuscript, is necessary to further the development of preventative and therapeutic strategies to combat allergic disease.

SUPPLEMENTARY DATA

Supplementary data are available at *Toxicological Sciences* online.

FUNDING

Internal funds from the Health Effects Laboratory Division of the National Institute for Occupational Safety and Health.

DECLARATION OF CONFLICTING INTERESTS

The authors declared no potential conflicts of interest with respect to the research, authorship, and/or publication of this article.

REFERENCES

Abais, J. M., Xia,2M., Zhang,2Y., Boini,2K. M., and Li,2P. L. (2015). Redox regulation of NLRP3 inflammasomes: ROS as trigger or effector? *Antioxid. Redox Signal.* **22**, 1111–1129.

Ahn, K. C., Zhao,2B., Chen,2J., Cherednichenko,2G., Sanmarti,2E., Denison,2M. S., Lasley,2B., Pessah,2I. N., Kultz,2D., Chang,2D. P., *et al.* (2008). *In vitro* biologic activities of the antimicrobials triclocarban, its analogs, and triclosan in bioassay screens: Receptor-based bioassay screens. *Environ. Health Perspect.* **116**, 1203–1210.

Allmyr, M., Adolfsson-Erici,2M., McLachlan,2M. S., and Sandborgh-Englund,2G. (2006). Triclosan in plasma and milk from Swedish nursing mothers and their exposure via personal care products. *Sci. Total Environ.* **372**, 87–93.

Allmyr, M., Harden,2F., Toms,2L. M., Mueller,2J. F., McLachlan,2M. S., Adolfsson-Erici,2M., and Sandborgh-Englund,2G. (2008). The influence of age and gender on triclosan concentrations in Australian human blood serum. *Sci. Total Environ.* **393**, 162–167.

Anderson, S. E., Franko,2J., Kashon,2M. L., Anderson,2K. L., Hubbs,2A. F., Lukomska,2E., and Meade,2B. J. (2013). Exposure to triclosan augments the allergic response to ovalbumin in a mouse model of asthma. *Toxicol. Sci.* **132**, 96–106.

Anderson, S. E., Meade,2B. J., Long,2C. M., Lukomska,2E., and Marshall,2N. B. (2016). Investigations of immunotoxicity and allergic potential induced by topical application of triclosan in mice. *J. Immunotoxicol.* **13**, 165–172.

Azzouz, A., Rascon,2A. J., and Ballesteros,2E. (2016). Simultaneous determination of parabens, alkylphenols, phenylphenols, bisphenol A and triclosan in human urine, blood and breast milk by continuous solid-phase extraction and gas chromatography-mass spectrometry. *J. Pharm. Biom. Anal.* **119**, 16–26.

Benani, A., Troy,2S., Carmona,2M. C., Fioramonti,2X., Lorsignol,2A., Leloup,2C., Casteilla,2L., and Penicaud,2L. (2007). Role for mitochondrial reactive oxygen species in brain lipid sensing: Redox regulation of food intake. *Diabetes* **56**, 152–160.

Besnard, A. G., Guillou,2N., Tschopp,2J., Erard,2F., Couillin,2I., Iwakura,2Y., Quesniaux,2V., Ryffel,2B., and Togbe,2D. (2011). NLRP3 inflammasome is required in murine asthma in the absence of aluminum adjuvant. *Allergy* **66**, 1047–1057.

Boro, M., and Balaji,2K. N. (2017). Cxcl1 and Cxcl2 regulate NLRP3 inflammasome activation via G-protein-coupled receptor Cxcr2. *J. Immunol. (Baltimore, MD: 1950)* **199**, 1660–1671.

Calafat, A. M., Ye,2X., Wong,2L. Y., Reidy,2J. A., and Needham,2L. L. (2008). Urinary concentrations of triclosan in the U.S. population: 2003–2004. *Environ. Health Perspect.* **116**, 303–307.

Chao, T., Wang,2H., and Ho,2P. C. (2017). Mitochondrial control and guidance of cellular activities of T cells. *Front. Immunol.* **8**, 473.

Clayton, E. M., Todd,2M., Dowd,2J. B., and Aiello,2A. E. (2011). The impact of bisphenol A and triclosan on immune parameters in the U.S. population, NHANES 2003–2006. *Environ. Health Perspect.* **119**, 390–396.

Compan, V., Baroja-Mazo,2A., Lopez-Castejon,2G., Gomez,2A. I., Martinez,2C. M., Angosto,2D., Montero,2M. T., Herranz,2A. S., Bazan,2E., Reimers,2D., *et al.* (2012). Cell volume regulation modulates NLRP3 inflammasome activation. *Immunity* **37**, 487–500.

Crinnion, W. J. (2010). The CDC fourth national report on human exposure to environmental chemicals: What it tells us about our toxic burden and how it assist environmental medicine physicians. *Altern. Med. Rev.* **15**, 101–109.

Del Dotto, V., Fogazza,2M., Carelli,2V., Rugolo,2M., and Zanna,2C. (2018). Eight human Opa1 isoforms, long and short: What are they for? *Biochim. Biophys. Acta Bioenerg.* **1859**, 263–269.

Dhillon, G. S., Kaur,2S., Pulicharla,2R., Brar,2S. K., Cledon,2M., Verma,2M., and Surampalli,2R. Y. (2015). Triclosan: Current status, occurrence, environmental risks and bioaccumulation potential. *Int. J. Environ. Res. Public Health* **12**, 5657–5684.

Ding, W. X., Li,2M., Biazik,2J. M., Morgan,2D. G., Guo,2F., Ni,2H. M., Goheen,2M., Eskelinen,2E. L., and Yin,2X. M. (2012). Electron microscopic analysis of a spherical mitochondrial structure. *J. Biol. Chem.* **287**, 42373–42378.

Drexler, S. K., Bonsignore,2L., Masin,2M., Tardivel,2A., Jackstadt,2R., Hermeking,2H., Schneider,2P., Gross,2O., Tschopp,2J., and Yazdi,2A. S. (2012). Tissue-specific opposing functions of the inflammasome adaptor ASC in the regulation of epithelial skin carcinogenesis. *Proc. Natl. Acad. Sci. U.S.A.* **109**, 18384–18389.

El-Hattab, A. W., Suleiman,2J., Almannai,2M., and Scaglia,2F. (2018). Mitochondrial dynamics: Biological roles, molecular machinery, and related diseases. *Mol. Genet. Metab.* **125**, 315–321.

Evavold, C. L., and Kagan,2J. C. (2018). How inflammasomes inform adaptive immunity. *J. Mol. Biol.* **430**, 217–237.

Fang, J. L., Stingley,2R. L., Beland,2F. A., Harrouk,2W., Lumpkins,2D. L., and Howard,2P. (2010). Occurrence, efficacy, metabolism, and toxicity of triclosan. *J. Environ. Sci. Health C Environ. Carcinog. Ecotoxicol. Rev.* **28**, 147–171.

Fang, J. L., Vanlandingham,2M., da Costa,2G. G., and Beland,2F. A. (2016). Absorption and metabolism of triclosan after application to the skin of B6C3F1 mice. *Environ. Toxicol.* **31**, 609–623.

FDA. (2016). Safety and effectiveness of consumer antiseptics; topical antimicrobial drug products for over-the-counter human use. Final rule. *Fed. Regist.* **81**, 61106–61130.

Fedoseeva, I. V., Pyatrikas,2D. V., Stepanov,2A. V., Fedyaeva,2A. V., Varakina,2N. N., Rusaleva,2T. M., Borovskii,2G. B., and Rikhvanov,2E. G. (2017). The role of flavin-containing enzymes in mitochondrial membrane hyperpolarization and ROS production in respiring *Saccharomyces cerevisiae* cells under heat-shock conditions. *Sci. Rep.* **7**, 2586.

Foell, D., Wittkowski,2H., Vogl,2T., and Roth,2J. (2007). S100 proteins expressed in phagocytes: A novel group of damage-associated molecular pattern molecules. *J. Leukoc. Biol.* **81**, 28–37.

Folletti, I., Siracusa,2A., and Paolocci,2G. (2017). Update on asthma and cleaning agents. *Curr. Opin. Allergy Clin. Immunol.* **17**, 90–95.

Fonseca, T. B., Sanchez-Guerrero,2A., Milosevic,2I., and Raimundo,2N. (2019). Mitochondrial fission requires Drp1 but not dynamins. *Nature* **570**, E34–42.

Geens, T., Neels,2H., and Covaci,2A. (2012). Distribution of bisphenol-A, triclosan and n-nonylphenol in human adipose tissue, liver and brain. *Chemosphere* **87**, 796–802.

Giedt, R. J., Pfeiffer,2D. R., Matzavinos,2A., Kao,2C. Y., and Alevriadou,2B. R. (2012). Mitochondrial dynamics and motility inside living vascular endothelial cells: Role of bioenergetics. *Ann. Biomed. Eng.* **40**, 1903–1916.

Goldberg, E. L., Asher,2J. L., Molony,2R. D., Shaw,2A. C., Zeiss,2C. J., Wang,2C., Morozova-Roche,2L. A., Herzog,2R. I., Iwasaki,2A., and Dixit,2V. D. (2017). Beta-hydroxybutyrate deactivates neutrophil NLRP3 inflammasome to relieve gout flares. *Cell Rep.* **18**, 2077–2087.

Groslambert, M., and Py,2B. F. (2018). Spotlight on the NLRP3 inflammasome pathway. *J. Inflamm. Res.* **11**, 359–374.

Gu, Y., Kuida,2K., Tsutsui,2H., Ku,2G., Hsiao,2K., Fleming,2M. A., Hayashi,2N., Higashino,2K., Okamura,2H., Nakanishi,2K., *et al.* (1997). Activation of interferon-gamma inducing factor mediated by interleukin-1beta converting enzyme. *Science (New York, NY)* **275**, 206–209.

He, Y., Franchi,2L., and Nunez,2G. (2013). TLR agonists stimulate NLRP3-dependent IL-1beta production independently of the purinergic P2X7 receptor in dendritic cells and *in vivo*. *J. Immunol. (Baltimore, MD: 1950)* **190**, 334–339.

He, Y., Hara,2H., and Nunez,2G. (2016). Mechanism and regulation of NLRP3 inflammasome activation. *Trends Biochem. Sci.* **41**, 1012–1021.

Heid, M. E., Keyel,2P. A., Kamga,2C., Shiva,2S., Watkins,2S. C., and Salter,2R. D. (2013). Mitochondrial reactive oxygen species induces NLRP3-dependent lysosomal damage and inflammasome activation. *J. Immunol. (Baltimore, MD: 1950)* **191**, 5230–5238.

The U.S. Department of Health and Human Services (HHS). (2001–2019). *Household Products Database of the National Library of Medicine*. Available at: https://www.nlm.nih.gov/toxnet/index.html; https://www.whatsinproducts.com/chemicals/view/1/95/003380-34-5/Triclosan.

Hong, S., Kwon,2H. J., Choi,2W. J., Lim,2W. R., Kim,2J., and Kim,2K. (2014). Association between exposure to antimicrobial household products and allergic symptoms. *Environ. Health Toxicol.* **29**, e2014017.

Huang, H., Du,2G., Zhang,2W., Hu,2J., Wu,2D., Song,2L., Xia,2Y., and Wang,2X. (2014). The *in vitro* estrogenic activities of triclosan and triclocarban. *J. Appl. Toxicol.* **34**, 1060–1067.

Iyer, S. S., He,2Q., Janczy,2J. R., Elliott,2E. I., Zhong,2Z., Olivier,2A. K., Sadler,2J. J., Knepper-Adrian,2V., Han,2R., Qiao,2L., *et al.* (2013). Mitochondrial cardiolipin is required for NLRP3 inflammasome activation. *Immunity* **39**, 311–323.

Jackson-Browne, M. S., Papandonatos,2G. D., Chen,2A., Calafat,2A. M., Yolton,2K., Lanphear,2B. P., and Braun,2J. M. (2018). Identifying vulnerable periods of neurotoxicity to triclosan exposure in children. *Environ. Health Perspect.* **126**, 057001.

Kanetoshi, A., Katsura,2E., Ogawa,2H., Ohyama,2T., Kaneshima,2H., and Miura,2T. (1992). Acute toxicity, percutaneous absorption and effects on hepatic mixed function oxidase activities of 2,4,4′-trichloro-2′-hydroxydiphenyl ether (Irgasan DP300) and its chlorinated derivatives. *Arch. Environ. Contam. Toxicol.* **23**, 91–98.

Klink, K. J., and Meade,2B. J. (2003). Dermal exposure to 3-amino-5-mercapto-1,2,4-triazole (AMT) induces sensitization and airway hyperreactivity in BALB/c mice. *Toxicol. Sci.* **75**, 89–98.

Li, Y., Zhou,2Z. H., Chen,2M. H., Yang,2J., Leng,2J., Cao,2G. S., Xin,2G. Z., Liu,2L. F., Kou,2J. P., Liu,2B. L., *et al.* (2016). Inhibition of mitochondrial fission and NOX2 expression prevent NLRP3 inflammasome activation in the endothelium: The role of corosolic acid action in the amelioration of endothelial dysfunction. *Antioxid. Redox Signal.* **24**, 893–908.

Liao, Y., Hussain,2T., Liu,2C., Cui,2Y., Wang,2J., Yao,2J., Chen,2H., Song,2Y., Sabir,2N., Hussain,2M., *et al.* (2019). Endoplasmic reticulum stress induces macrophages to produce IL-1beta during *Mycobacterium bovis* infection via a positive feedback loop between mitochondrial damage and inflammasome activation. *Front. Immunol.* **10**, 268.

Liu, P., Xie,2Q., Wei,2T., Chen,2Y., Chen,2H., and Shen,2W. (2015). Activation of the NLRP3 inflammasome induces vascular dysfunction in obese OLETF rats. *Biochem. Biophys. Res. Commun.* **468**, 319–325.

Liu, Q., Zhang,2D., Hu,2D., Zhou,2X., and Zhou,2Y. (2018). The role of mitochondria in NLRP3 inflammasome activation. *Mol. Immunol.* **103**, 115–124.

MacIsaac, J. K., Gerona,2R. R., Blanc,2P. D., Apatira,2L., Friesen,2M. W., Coppolino,2M., and Janssen,2S. (2014). Health care worker exposures to the antibacterial agent triclosan. *J. Occup. Environ. Med.* **56**, 834–839.

Mariathasan, S., Weiss, D. S., Newton, K., McBride, J., O'Rourke, K., Roose-Girma, M., Lee, W. P., Weinrauch, Y., Monack, D. M., and Dixit, V. M. (2006). Cryopyrin activates the inflammasome in response to toxins and ATP. *Nature* **440**, 228–232.

Marshall, N. B., Lukomska,2E., Long,2C. M., Kashon,2M. L., Sharpnack,2D. D., Nayak,2A. P., Anderson,2K. L., Jean Meade,2B., and Anderson,2S. E. (2015). Triclosan induces thymic stromal lymphopoietin in skin promoting Th2 allergic responses. *Toxicol. Sci.* **147**, 127–139.

Marshall, N. B., Lukomska,2E., Nayak,2A. P., Long,2C. M., Hettick,2J. M., and Anderson,2S. E. (2017). Topical application of the anti-microbial chemical triclosan induces immunomodulatory responses through the S100A8/A9-TLR4 pathway. *J. Immunotoxicol.* **14**, 50–59.

Martinon, F. (2010). Signaling by ROS drives inflammasome activation. *Eur. J. Immunol.* **40**, 616–619.

Merkwirth, C., and Langer,2T. (2009). Prohibitin function within mitochondria: Essential roles for cell proliferation and cristae morphogenesis. *Biochim. Biophys. Acta* **1793**, 27–32.

Moss, T., Howes,2D., and Williams,2F. M. (2000). Percutaneous penetration and dermal metabolism of triclosan (2,4,4′-trichloro-2′-hydroxydiphenyl ether). Food and chemical toxicology: An international journal published for the British Industrial. *Biol. Res. Assoc.* **38**, 361–370.

Munoz-Planillo, R., Kuffa,2P., Martinez-Colon,2G., Smith,2B. L., Rajendiran,2T. M., and Nunez,2G. (2013). $K^{(+)}$ efflux is the common trigger of NLRP3 inflammasome activation by bacterial toxins and particulate matter. *Immunity* **38**, 1142–1153.

Palmer, R. K., Hutchinson, L. M., Burpee, B. T., Tupper, E. J., Pelletier, J. H., Kormendy, Z., Hopke, A. R., Malay, E. T., Evans, B. L., Velez, A., *et al.* (2012). Antibacterial agent triclosan suppresses RBL-2H3 mast cell function. *Toxicol. Appl. Pharmacol.* **258**, 99–108.

Park, S., Won,2J. H., Hwang,2I., Hong,2S., Lee,2H. K., and Yu,2J. W. (2015). Defective mitochondrial fission augments NLRP3 inflammasome activation. *Sci. Rep.* **5**, 15489.

Pearce, E. L., Poffenberger,2M. C., Chang,2C. H., and Jones,2R. G. (2013). Fueling immunity: Insights into metabolism and lymphocyte function. *Science (New York, NY)* **342**, 1242454.

Pedra, J. H., Cassel,2S. L., and Sutterwala,2F. S. (2009). Sensing pathogens and danger signals by the inflammasome. *Curr. Opin. Immunol.* **21**, 10–16.

Perregaux, D., and Gabel,2C. A. (1994). Interleukin-1 beta maturation and release in response to ATP and nigericin. Evidence that potassium depletion mediated by these agents is a necessary and common feature of their activity. *J. Biol. Chem.* **269**, 15195–15203.

Ruby Pawankar, G. W. C., Holgate, S. T., and Lockey, R. F. (2012). The WAO White Book on Allergy 2011–2012. World Health Organization.

Sagoo, P., Garcia,2Z., Breart,2B., Lemaitre,2F., Michonneau,2D., Albert,2M. L., Levy,2Y., and Bousso,2P. (2016). *In vivo* imaging of inflammasome activation reveals a subcapsular macrophage burst response that mobilizes innate and adaptive immunity. *Nat. Med.* **22**, 64–71.

Sand, J., Haertel,2E., Biedermann,2T., Contassot,2E., Reichmann,2E., French,2L. E., Werner,2S., and Beer, H. D. (2018). Expression of inflammasome proteins and inflammasome activation occurs in human, but not in murine keratinocytes. *Cell Death Dis.* **9**, 24.

Sasseville, D. (2008). Occupational contact dermatitis. *Allergy Asthma Clin. Immunol.* **4**, 59–65.

Savage, J. H., Johns,2C. B., Hauser,2R., and Litonjua,2A. A. (2014). Urinary triclosan levels and recent asthma exacerbations. *Ann. Allergy Asthma Immunol.* **112**, 179–181.e172.

Savage, J. H., Matsui,2E. C., Wood,2R. A., and Keet,2C. A. (2012). Urinary levels of triclosan and parabens are associated with aeroallergen and food sensitization. *J. Allergy Clin. Immunol.* **130**, 453–460.e457.

Shane, H. L., Long,2C. M., and Anderson,2S. E. (2019). Novel cutaneous mediators of chemical allergy. *J. Immunotoxicol.* **16**, 13–15.

Sharma, D., and Kanneganti,2T. D. (2016). The cell biology of inflammasomes: Mechanisms of inflammasome activation and regulation. *J. Cell Biol.* **213**, 617–629.

Shim, J., Weatherly,2L. M., Luc,2R. H., Dorman,2M. T., Neilson,2A., Ng,2R., Kim,2C. H., Millard,2P. J., and Gosse,2J. A. (2016). Triclosan is a mitochondrial uncoupler in live zebrafish. *J. Appl. Toxicol.* **36**, 1662–1667.

Simard, J. C., Cesaro,2A., Chapeton-Montes,2J., Tardif,2M., Antoine,2F., Girard,2D., and Tessier,2P. A. (2013). S100A8 and s100A9 induce cytokine expression and regulate the NLRP3 inflammasome via ROS-dependent activation of NF-kappaB(1). *PLoS One* **8**, e72138.

Spanier, A. J., Fausnight,2T., Camacho,2T. F., and Braun,2J. M. (2014). The associations of triclosan and paraben exposure with allergen sensitization and wheeze in children. *Allergy Asthma Proc.* **35**, 475–481.

Stoker, T. E., Gibson,2E. K., and Zorrilla,2L. M. (2010). Triclosan exposure modulates estrogen-dependent responses in the female Wistar rat. *Toxicol. Sci.* **117**, 45–53.

Szychowski, K. A., Wnuk,2A., Kajta,2M., and Wójtowicz,2A. K. (2016). Triclosan activates aryl hydrocarbon receptor (AhR)-dependent apoptosis and affects Cyp1a1 and Cyp1b1 expression in mouse neocortical neurons. *Environ. Res.* **151**, 106–114.

Tamura, I., Kanbara,2Y., Saito,2M., Horimoto,2K., Satoh,2M., Yamamoto,2H., and Oyama,2Y. (2012). Triclosan, an antibacterial agent, increases intracellular $Zn^{(2+)}$ concentration in rat thymocytes: Its relation to oxidative stress. *Chemosphere* **86**, 70–75.

Teplova, V. V., Belosludtsev,2K. N., and Kruglov,2A. G. (2017). Mechanism of triclosan toxicity: Mitochondrial dysfunction including complex II inhibition, superoxide release and uncoupling of oxidative phosphorylation. *Toxicol. Lett.* **275**, 108–117.

Thornberry, N. A., Bull,2H. G., Calaycay,2J. R., Chapman,2K. T., Howard,2A. D., Kostura,2M. J., Miller,2D. K., Molineaux,2S. M., Weidner,2J. R., and Aunins,2J. (1992). A novel heterodimeric cysteine protease is required for interleukin-1 beta processing in monocytes. *Nature* **356**, 768–774.

Toichi, E., Lu,2K. Q., Swick,2A. R., McCormick,2T. S., and Cooper,2K. D. (2008). Skin-infiltrating monocytes/macrophages migrate to draining lymph nodes and produce IL-10 after contact sensitizer exposure to UV-irradiated skin. *J. Invest. Dermatol.* **128**, 2705–2715.

van der Windt, G. J., and Pearce,2E. L. (2012). Metabolic switching and fuel choice during T-cell differentiation and memory development. *Immunol. Rev.* **249**, 27–42.

Wang, L., Asimakopoulos,2A. G., and Kannan,2K. (2015). Accumulation of 19 environmental phenolic and xenobiotic heterocyclic aromatic compounds in human adipose tissue. *Environ. Int.* **78**, 45–50.

Wang, X., Jiang,2W., Yan,2Y., Gong,2T., Han,2J., Tian,2Z., and Zhou,2R. (2014). RNA viruses promote activation of the NLRP3 inflammasome through a RIP1-RIP3-DRP1 signaling pathway. *Nat. Immunol.* **15**, 1126–1133.

Weatherly, L. M., and Gosse,2J. A. (2017). Triclosan exposure, transformation, and human health effects. *J. Toxicol. Environ. Health B Crit. Rev.* **20**, 447–469.

Weatherly, L. M., Nelson,2A. J., Shim,2J., Riitano,2A. M., Gerson,2E. D., Hart,2A. J., de Juan-Sanz,2J., Ryan,2T. A., Sher,2R., Hess,2S. T., *et al.* (2018). Antimicrobial agent triclosan disrupts mitochondrial structure, revealed by super-resolution microscopy, and inhibits mast cell signaling via calcium modulation. *Toxicol. Appl. Pharmacol.* **349**, 39–54.

Weatherly, L. M., Shim,2J., Hashmi,2H. N., Kennedy,2R. H., Hess,2S. T., and Gosse,2J. A. (2016). Antimicrobial agent triclosan is a proton ionophore uncoupler of mitochondria in living rat and human mast cells and in primary human keratinocytes. *J. Appl. Toxicol.* **36**, 777–789.

Wei, L., Qiao,2P., Shi,2Y., Ruan,2Y., Yin,2J., Wu,2Q., and Shao,2B. (2017). Triclosan/triclocarban levels in maternal and umbilical blood samples and their association with fetal malformation. *Clin. Chim. Acta* **466**, 133–137.

West, A. P., Shadel,2G. S., and Ghosh,2S. (2011). Mitochondria in innate immune responses. *Nat. Rev. Immunol.* **11**, 389–402.

Won, J. H., Park,2S., Hong,2S., Son,2S., and Yu,2J. W. (2015). Rotenone-induced impairment of mitochondrial electron transport chain confers a selective priming signal for NLRP3 inflammasome activation. *J. Biol. Chem.* **290**, 27425–27437.

Woolhiser, M. R., Munson,2A. E., and Meade,2B. J. (2000). Comparison of mouse strains using the local lymph node assay. *Toxicology* **146**, 221–227.

Xiao, Y., Xu,2W., and Su,2W. (2018). NLRP3 inflammasome: A likely target for the treatment of allergic diseases. *Clin. Exp. Allergy* **48**, 1080–1091.

Yang, Y., Wang,2H., Kouadir,2M., Song,2H., and Shi,2F. (2019). Recent advances in the mechanisms of NLRP3 inflammasome activation and its inhibitors. *Cell Death Dis.* **10**, 128.

Yu, J. W., and Lee,2M. S. (2016). Mitochondria and the NLRP3 inflammasome: Physiological and pathological relevance. *Arch. Pharm. Res.* **39**, 1503–1518.

Yueh, M. F., Taniguchi,2K., Chen,2S., Evans,2R. M., Hammock,2B. D., Karin,2M., and Tukey,2R. H. (2014). The commonly used antimicrobial additive triclosan is a liver tumor promoter. *Proc. Natl. Acad. Sci. U.S.A.* **111**, 17200–17205.

Zhang, P., Yang,2M., Zeng,2L., and Liu,2C. (2018). P38/TRHr-dependent regulation of TPO in thyroid cells contributes to the hypothyroidism of triclosan-treated rats. *Cell. Physiol. Biochem.* **45**, 1303–1315.

Zhang, X., Zhang,2X., Zhang,2Y., Liu,2M., Jin,2J., Yan,2J., Shen,2X., Hu,2N., and Dong,2D. (2017). Mitochondrial uncoupler triclosan induces vasorelaxation of rat arteries. *Acta Pharm. Sin. B* **7**, 623–629.

Zhou, R., Yazdi,2A. S., Menu,2P., and Tschopp,2J. (2011). A role for mitochondria in NLRP3 inflammasome activation. *Nature* **469**, 221–225.

Zorov, D. B., Juhaszova,2M., and Sollott,2S. J. (2006). Mitochondrial ROS-induced ROS release: An update and review. *Biochim. Biophys. Acta* **1757**, 509–517.